

Femtosecond Laser Eyewear Protection: Measurements and Precautions for Amplified High Power Applications

**Maximilian Riedel-Topper,¹ Sarah Wirick,¹ Joshua A. Hadler,² Brian G. Alberding³
Christopher J. Stromberg¹ and Edwin J. Heilweil³**

¹Department of Chemistry and Physics, Hood College, 401 Rosemont Ave, Frederick, MD 21710

²Applied Physics Division, Physical Measurement Laboratory, NIST Boulder, CO 80305

³Engineering Physics Division, Physical Measurement Laboratory, NIST Gaithersburg, MD 20899

Abstract

Ultrafast lasers have become increasingly important as research tools in laboratories and commercial enterprises suggesting laser safety, personal protection and awareness become ever more important. Laser safety eyewear are typically rated by their optical densities (OD) over various spectral ranges, but these measurements are usually made using low power, large beam size, and continuous beam conditions. These measurement scenarios are vastly different than the high power, small beam size, and pulsed laser beam conditions where ultrafast lasers have extremely high peak powers and broad spectra due to the short pulse durations. Many solid-state lasers are also tunable over a broad wavelength range, further complicating the selection of adequate laser safety eyewear. Eighteen laser eyewear filter samples were tested under real-world conditions using a Ti:Sapphire regenerative amplifier with output pulses centered at 800 nm running from 2 Hz to 1 KHz repetition rate. The typical maximum peak laser irradiance employed was ca. 3 TW/cm² (800 nm wavelength, 450 uJ/pulse with 80 fs FWHM pulse duration) or less when damage occurred, depending on the sample. While many samples maintained their integrity under these test conditions, many plastic samples showed signs of failure which reduced their OD, in some cases transmitting 4 to 5 orders of magnitude higher than expected. In general, glass filters performed significantly better than plastic filters, exhibiting less physical damage to the substrate and less absorber degradation.

Key words: femtosecond lasers; laser safety eyewear protection; optical density specifications; ultra-high peak power; failure modes; ultrafast lasers

I. INTRODUCTION

Femtosecond pulsed lasers are increasingly being used in research and commercial applications. Unlike continuous-wave lasers, femtosecond lasers ($<10^{-13}$ s pulse durations) have intrinsically wide spectral bandwidths and extremely high peak irradiances, readily attaining TW/cm^2 levels. Lasers such as Ti:Sapphire oscillators also have an adjustable center wavelength. These factors become an issue when selecting eyewear protection, as the eyewear may not protect the user from the entire laser spectrum and the integrity of the eyewear material may be compromised by the employed high peak powers. Additionally, laser eyewear protection is typically tested by using a low power light source or spectrophotometers to measure spectral absorption, so the manufacturer's specifications may not be adequate indicators of the eyewear's level of protection for the broadband output of pulsed laser systems. Therefore, it is imperative to determine (1) the efficacy of the laser eyewear protection under actual experimental conditions and (2) the potential modes of failure. The high peak power experiments discussed in this work are a follow-on to a previous study¹ that measured the effective optical densities (ODs) of several commercial laser eyewear samples, using the same samples investigated here, under much lower irradiance conditions. Earlier investigations using similar amplified laser output were performed, but only a few known studies were conducted and samples previously investigated by others.²

II. METHODS

A. Ti^{+3} :Sapphire Amplified Femtosecond Apparatus

A home-built 1 kHz Ti:Sapphire regenerative amplifier was seeded by grating-stretched pulses from a mode-locked Ti:Sapphire oscillator (pumped by a Coherent Lasers CW Verdi V laser running at 3.5 Watts) that generated ~ 30 fs pulses at 80 MHz with average output power of ~ 160 mW (Kapteyn-Murnane Lasers, Inc.).⁴ The amplifier was pumped by a Spectra Physics Empower 20 laser operating at 1

KHz with about 15 Watts average output power. The resulting amplified laser output, after pulse compression using dielectric mirrors and a four-pass gold grating, was centered at 800 nm with a bandwidth of 25 nm full width at half maximum (FWHM), pulse duration of 80 fs FWHM and average maximum delivered power to the sample under test of ~450 mW. A schematic diagram of the laser and optical setup used is shown in Figure 1.

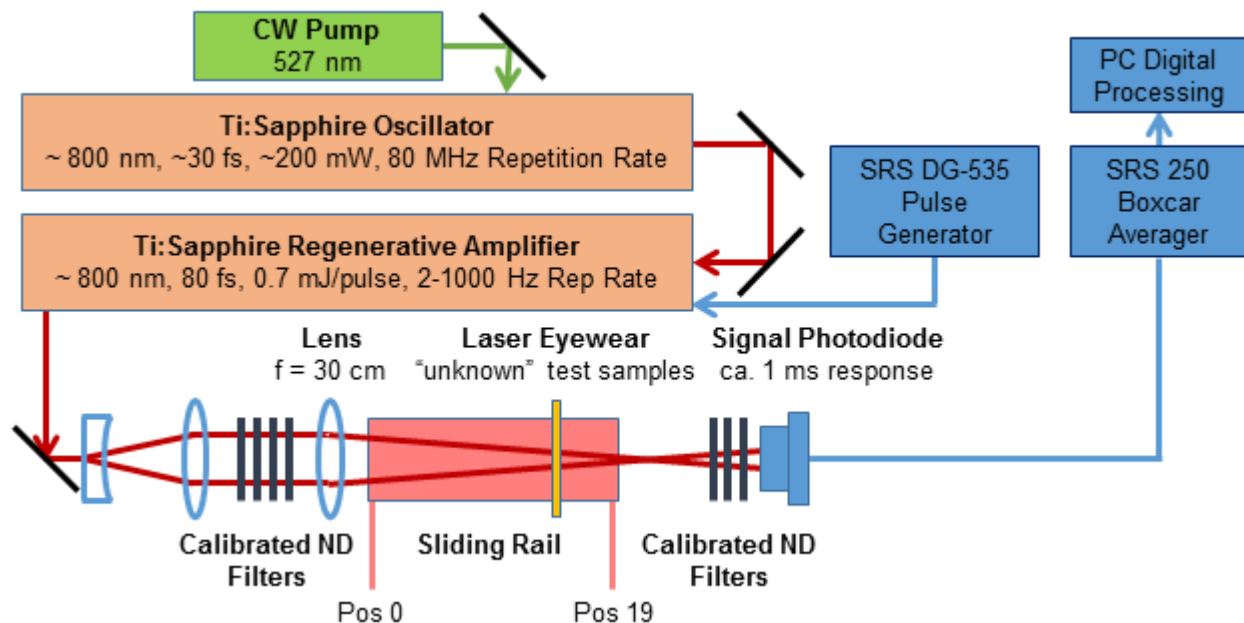


Figure 1. Schematic of laser system used to measure transmission through laser safety eyewear.

B. Eyewear Samples and Experimental Method

Eyewear samples were kindly donated by five laser safety eyewear manufacturers. A total of 18 samples were tested with the nominally 800 nm regenerative amplifier center wavelength output at varying spot sizes and amplifier repetition rates. Samples are referred to by arbitrarily assigned letters to maintain the manufacturers' anonymity (Note: sample labels A through V are consistent with Ref. 1). Examples of the tested eyewear and samples are provided in the Supplemental Information (Figures S1 and S2). The amplifier output beam was expanded and collimated to a diameter of about 2.5 cm so that calibrated neutral density (ND) filters could be inserted in the collimated beam path to control the laser power. An $f = 30$ cm focal length positive lens subsequently focused the beam to provide a smoothly

varying beam diameter at the sample position. The eyewear samples were held by an optical mount that could be moved along a sliding rail parallel to the path of the laser beam. The position furthest from the detector was labeled as Position 0, and positions beyond that were measured in centimeters from Position 0 up to 19, which was closest to the focal point of the laser. After each laser exposure, the sample was moved to a new focal position (exposing the same area) and in some cases, a series of repetition rates to monitor cumulative effects. A large aperture silicon PIN photodiode (1 cm x 1 cm) producing un-amplified voltage output was used as the detector to minimize beam spatial and positional artifacts.

The laser pulse repetition rate could be set to the maximum 1 KHz and lower values of the regenerative amplifier by inserting precision millisecond time delays (Stanford Research Systems SRS DG-535 pulse generator) between pulses that controlled the Q-switched single intracavity Pockels cell. This allowed for the samples to be tested at pulse repetition rates as low as 2 Hz. The laser beam profile was measured at each sample position using a large format CCD camera and sampling electronics before analyzing the eyewear samples to determine if it varied with different repetition rates (see Figures S3 to S7). In this way, beam spot size and radiant exposures were verified to not be significantly affected by changes in repetition rate. A compilation of measured pulsed beam parameters including orthogonal diameters and estimated maximum peak irradiance at the various sample positions is provided in Table 1.

Table 1. Beam diameters (FWHM) and maximum peak pulse irradiance for various sample positions (without ND filters before sample) with 450 mW average incident power. Beam diameters were extracted from fits to a Gaussian profile (see Figs S3-S7 below). Reported estimated error values (σ) are for both the x and y dimensions. Values and standard deviations are given for the beams with the laser running at repetition rates of 2, 50, 100, 200, 500, and 1000 Hz.

Position	Diameter x (mm)	Diameter y (mm)	Max. Peak Irradiance (GW/cm ²) ^a
14.0	1.7 ± 0.11	1.9 ± 0.26	210
16.5	1.14 ± 0.048	1.3 ± 0.12	457
17.5	0.85 ± 0.055	0.99 ± 0.057	803
18.25	0.62 ± 0.036	0.78 ± 0.042	1400
19.0	0.41 ± 0.023	0.58 ± 0.021	2700

^a Estimated from full power, average of x and y beam dimensions, and pulse duration

Detector signals (Volts at photodiode output waveform maximum) were sampled by a boxcar averager (SRS 250 Stanford Research Systems) with appropriate gain to maintain linearity (maximum 5 Volt output) and digitized on each shot for computer data acquisition. When required, calibrated ND filters (each nominally OD=1 referred to as Filters 1, 2 and 3 below) placed before the detector were inserted in the beam path to maintain detector linearity. Background signals, originating from sources such as room light offsets, were eliminated from the sampled transmitted pulsed data by collecting and subtracting a blank sample before each test pulse. To measure “laser off” light background levels, an aluminum plate was placed far up-stream from the detection optics to block the laser from passing through the sample and reaching the detector. The average background signal at each set of conditions was then subtracted from each data point collected under those conditions to obtain the analyzed signal levels presented and discussed below. Average values were typically extracted by measuring five hundred to one thousand laser pulses (with ca. $\pm 10\%$ deviation, type b, $k=1$ analysis).

III. RESULTS

In this study, five different modes of failure or no failure were observed for the laser eyewear samples tested. Five types of repetition rate dependencies were also found during testing, although not all were observed for all samples tested. Categorization of the types of failure and repetition rate dependencies is given below, followed by a summary (see Table 2) of the results for each sample tested. A selection of samples exhibiting the five modes of failure are also discussed within this section.

A. Classification of Failure and no Failure Modes:

1. **Saturable Absorber** – Signal increases based on focus position/power, but no visible damage observed. The sample recovers to its original absorbance value under very low irradiance.
2. **Bleaching/Damage to Dye** – Signal increases based on focus position/power. Visible irreversible damage occurs to the dye, either loss of dye or color change. No damage to the substrate is observable.

3. **Melting** – Signal increases based on focus position/power. Visible permanent damage to the substrate (e.g, deformation/melted appearance) occurs.
4. **Burning** – Signal decreases (often after a transient increase from melting and/or bleaching). Visible damage/blackening of the substrate is observed.
5. **No Damage:** No failure observed under any studied conditions.

B. Repetition Rate Failure Dependence:

- A. Failure/Damage is cumulative and does not depend on repetition rate (slope of time-dependent transmission curve remains constant with varying repetition rates).
- B. Failure/Damage is cumulative and depends on repetition rate (slope of time-dependent transmission curve varies with repetition rate).
- C. Failure/Damage occurs too quickly to determine (via measurement signal voltage change).
- D. Failure/Damage is not cumulative, failure depends on repetition rate(via measurement signal voltage change).
- E. Failure/Damage is not cumulative, failure does not depend on repetition rate (via measurement signal voltage change).
- F. No repetition rate dependence, damage or failure

Table 2. Summary of data for the laser eyewear samples tested at various repetition rates and beam spot sizes at 800 nm. Failure modes and repetition rate dependencies annotated are defined above:

Sample	Supplier OD^a	Thickness (mm)^b	Material	OD^c	Failure Mode	Rep. Rate Dependence	Notes
A	>7	3.2	Glass	9.07	5	F	No damage.
C	7+	3.5	Glass	7.78	5	F	No damage.
D	7+	7.0	Glass	7.83	5	F	No damage.
E	7+	3.5	Glass	9.07	5	F	No damage.
F	2	3.2	Acrylic	3.5	2	B	Continually let through more light as rep rate was increased at Position 16.5. Visibly bleached at Position 16.5 at 1 kHz.
G	7+	3.0	Poly carbonate	7.38	3→4	B	Began melting at Position 17 at 1 kHz. Burned at Position 19 at 1 kHz.
H	5+	2.0	Poly carbonate	1.23	3→4	E→B	Very low measured OD; found to not be a good sample for this pulsed-laser experiment.
I		2.0	Poly carbonate	8.18	3→4	E→B	Let through light while visibly melting, but quickly turned over to burning at Position 18.25 at 1 kHz.
J	>7	6.2	Glass	8.15	5	F	No damage.
K	>6	3.4	Glass	7.92	5	F	No damage.
L	>6	4.0	Glass	8.88	5	F	No damage.
M	7+	3.0	Poly carbonate	7.38	3→4	B	Melting and saturation didn't occur until tightly focused at Position 19. Visibly burned after several consecutive runs at Position 19 at 1 kHz.

N	5+	3.0	Poly carbonate	5.44	1→2	E→A	Bleached with full power of laser at Position 19; unrecoverable.
O	5+	3.2	Poly carbonate	3.16	2	A	Bleached then saturated detector at Position 19.
P	7+	3.0	Poly carbonate	9.05	3→4	B	Near infinite absorber. Visible damage started at Position 17.5 at 1 kHz, but no increase in signal until Position 19. Burned at Position 19 at 500 Hz.
Q	6+	3.2	Poly carbonate	8.85	3→4	B	Near infinite absorber. Visible melting started at Position 18.25 and allowed ~5 orders of magnitude more light through at 500 Hz. Completely burned after three runs at 1 kHz.
R	7+	3.0	Poly carbonate	7.44	3→4	B	Visible melting at Position 16.5. At Position 19, allowed ~5 orders of magnitude more light through with Filters 1, 2, and 3. Burned at Position 19 at 500 Hz.
U	7+	2.0	Poly carbonate	7.33	3→4	B	Started melting at Position 16.5 at 1 kHz. Slowly let through less light as rep rate increased at Position 18.25. Completely burned at Position 19 at 2 Hz.
V		2.0	Poly carbonate	7.47	1→3→4	E→A	Let a little more light through at Position 16.5, but not cumulative. Visibly damaged at Position 16.5 at 1 kHz. Burned at Position 19 at 1 kHz.

^aOptical Density at 800 nm center wavelength provided by supplier with sample or from website

^b Nominally measured thickness of sample (mm).

^c Measured Optical Density at low CW irradiance levels found in Ref. 1.

IV. DISCUSSION

We present and discuss here a few examples of sample behavior presented in Table 1 that exhibited no sign of damage or significant changes when exposed to various laser irradiance conditions. Sample K is an example of a filter that showed no sign of damage or failure under any of the conditions tested.² Its performance was unchanged regardless of the spot size and applied repetition rate conditions, even under illumination with the full 450 mW average power (e.g., 2.7 TW/cm² maximum peak irradiance). A graph of the signal (in Volts) at each repetition rate and position for Sample K is shown in Figure 2.

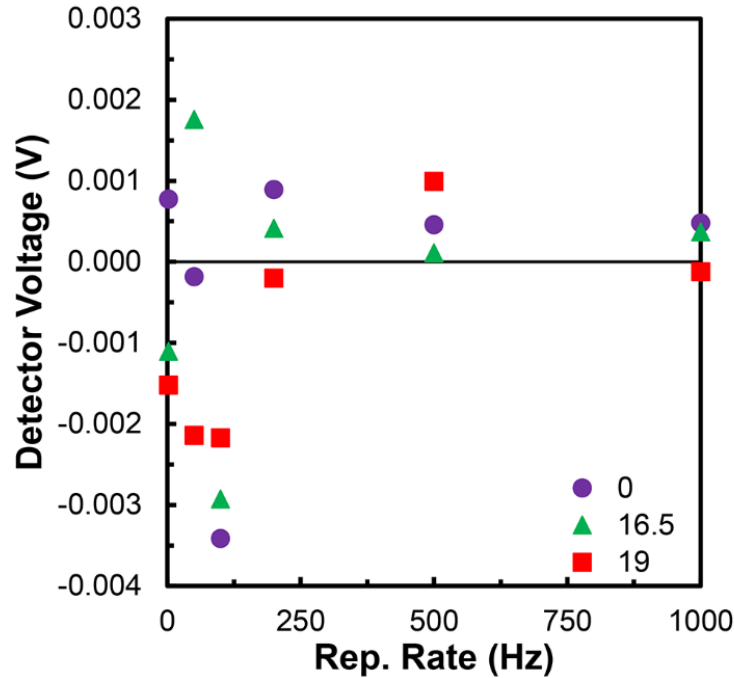


Figure 2. Measured signal (Volts) at different repetition rates (Hz) and positions for Sample K. The sample positions (cm from start of rail) are listed in the right-hand legend. The transmitted light for this sample at various positions and pulse irradiance are negligible and represent noise on the measurement. The differences in signal between repetition rate and spot sizes are all within the standard deviation of individual laser shots (± 0.0043 V). This sample was nearly opaque at the center wavelengths employed,

with a measured OD of 7.92 at 800 nm center wavelength and the OD of this sample exceeded the measurement capability of our system

Sample F is an example of a sample that bleached without incurring any visible damage to the substrate itself. As the irradiance increased, the transmitted signal increased. A graph displaying the change in signal at each shot number and repetition rate for Sample F at Position 16.5 is shown in Figure 3. At 2 Hz and 50 Hz repetition rate, attenuating Filter 1 was placed before the detector to maintain detector linearity and additional filters were placed before the detector for higher repetition rates. At 100 Hz, 200 Hz, 500 Hz and the first two runs at 1 KHz (labelled as 1000(1) and 1000(2) in the legend of Figure 3), Filters 1 and 2 were placed before the detector. The third filter was required for 1 KHz repeat runs 1000(3) and 1000(4) shown in Figure 3(c).

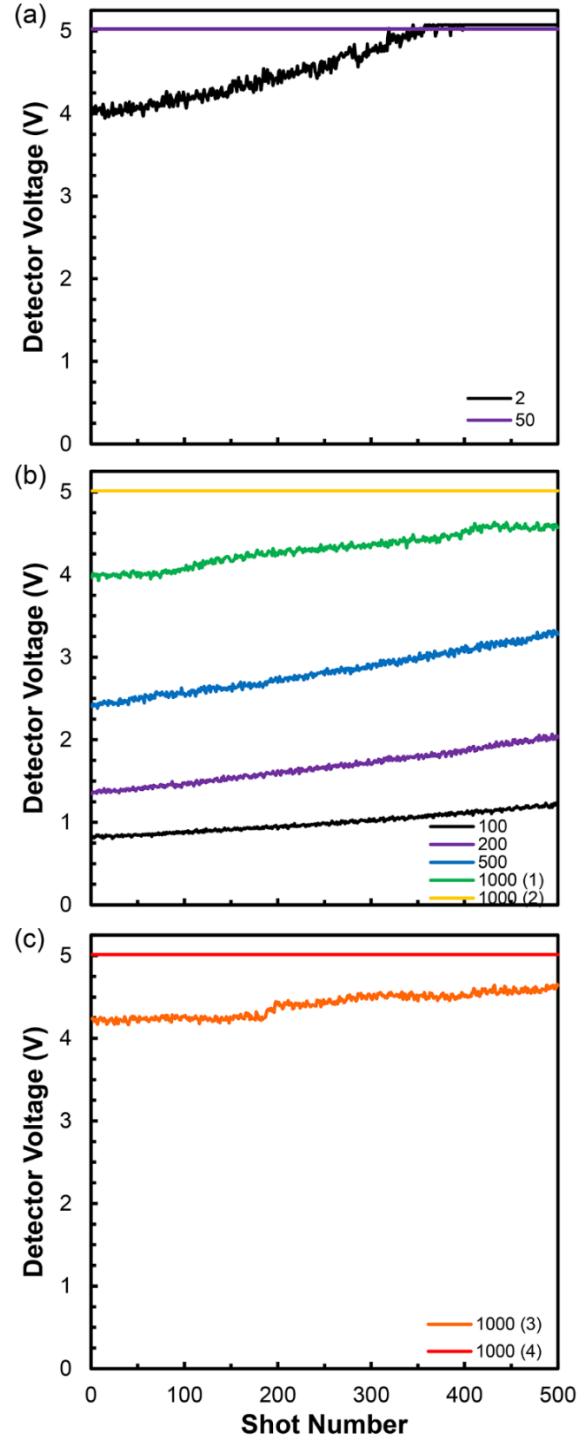


Figure 3. The measured detector signal in Volts (along the y-axis) of each laser pulse (along the x-axis) for Sample F fixed at Position 16.5 at various repetition rates (Hz) listed in the legend. Scans were taken successively with (a) one filter after the sample, (b) two filters after the sample, and (c) three ND=1 filters before the detector to reduce the transmitted signal below the 5 Volt saturation level.

For the remaining two runs at 1 KHz (labelled as 1000(3) and 1000(4) in the legend of Figure 3), Filters 1, 2, and 3 were placed in front of the detector. The runs at 50 Hz and the second and fourth run at 1 KHz repetition rate saturated the boxcar sampling at 5 V while the four runs at 1 KHz were completed consecutively. Although the sample transmitted more light at each repetition rate, bleaching occurred immediately at the outset of pulsed exposure at 1 KHz repetition rate. Figure 3 also indicates that the sample incurred cumulative damage, since the final signal from one run overlaps the initial signal of the following run. This trend occurred for repetition rates between 100 Hz, 200 Hz and 500 Hz.

Sample G is an example of a sample that melted and then burned at the smallest employed beam spot sizes. In a similar fashion as Sample F, the signal increased as the spot size decreased. A graph describing the signal at different repetition rates and positions for Sample G is shown in Figure 4. In Figure 4, the colors of the data points indicate the number of filters (Filters 1, 2 and 3) placed before the detector (green, yellow, orange, and red represent 0, 1, 2, and 3 filters, respectively).

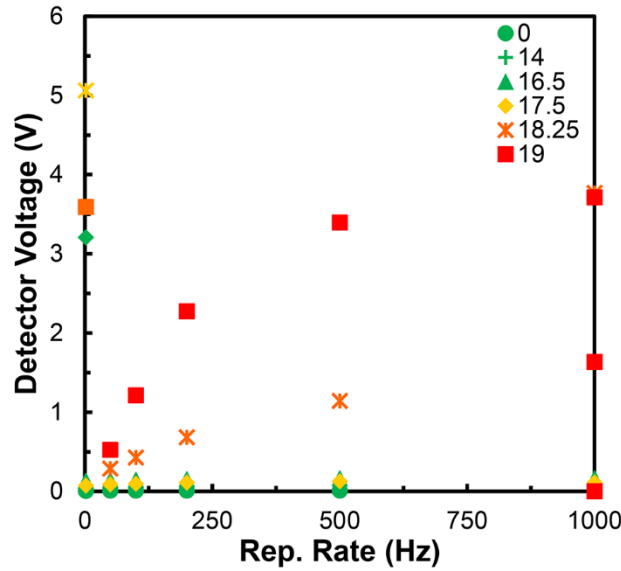


Figure 4. The measured signal in Volts (along the y-axis) at different repetition rates in Hz (along the x-axis) and sample positions (right-hand legend) for Sample G. Colors of points designate the number of OD = 1 filters placed before the detector (green, yellow, orange, and red represent the number 0, 1, 2, and 3 filters, respectively). Shapes of points represent the sample position as shown in the legend. Position 19 is closest to the beam focus.

Filter 2 was placed behind Sample G after the first run at positions 17.5 and 2 to protect the detector from nonlinear output and damage, and no damage was visible on the sample after these exposures. Sample G began visibly melting at 1 KHz repetition rate for position 17.5, but melting was noted to not visibly change as the experiment continued. Filter 1 was added in addition to Filter 2 behind the sample after the run at position 18.25 cm and 2 Hz because the signal reached the maximum limit and continued testing of the sample was needed to determine if burning and charring occurred. Three runs at position 19 cm and repetition rate 1 KHz were conducted in succession. The signal dropped from 3.71 V to 1.63 V, and finally to 0 V. This signal level change agrees with the concurrent visible observation of sample burning. After continual exposure to the laser beam, this sample eventually burned and charred to the extent that it blocked all laser light.

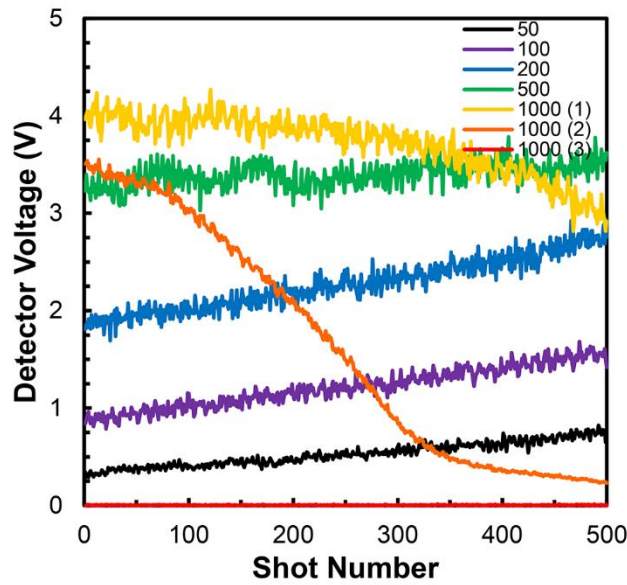


Figure 5. The measured transmitted signal (Volts) for each successive laser pulse for Sample G at Position 19 at repetition rates (Hz) listed in the legend.

Figure 5 shows the change in signal during each run at Position 19 for Sample G. The slopes of the curve for each repetition rate differ, indicating that sample damage depends on the repetition rate. The rate of increased signal at 50 Hz was about half the rate as for 100 Hz and 200 Hz. The rate of increased signal was lowest at 500 Hz, possibly since the sample was approaching burning. In a similar fashion as

Sample F, Sample G incurred cumulative damage. This trend is clearly visible for all repetition rates, since the final signal of one run was approximately at the same initial signal level for the following run. Signal levels increased rapidly from 50 Hz up to 500 Hz repetition rates, indicating that the sample melted during all runs. Burning occurs even for the first run at 1 KHz, where the signal starts to rapidly decrease. During the following run, the rate of burning increased six-fold before leveling off at around shot number 300. By the final run, the sample was completely burned and blocked all light.

An example of a sample that acts as a saturable absorber under relatively low peak irradiance conditions is Sample N (see Figure S2). A graph of the transmitted signal at each repetition rate and position for Sample N is shown in Figure 6 (Note: these data were taken with one neutral density filter placed before the sample, resulting in an incident average power of 60 mW and estimated maximum peak irradiance of 400 GW/cm² at sample Position 19 with 1 KHz repetition rate). At each position, the signal remained relatively constant. However, as the laser irradiance increased, the amount of light transmitted through to the detector increased. The measured signal level was directly related to the sample position, and when the sample was moved back to a larger beam diameter, its transmission would return to its original absorbance level. At higher irradiance, the effective OD decreased. However, these results indicate that the sample can recover its transmissive properties when exposed at the larger spot sizes. Additionally, the amount of light transmitted to the detector did not significantly change over the course of any run at any sample position. Permanent damage did not occur until testing Sample N at Position 19. The sample did not melt, but the green color of the dye in the beam path noticeably and permanently decreased. This overall behavior indicates that the sample is a saturable absorber even at larger spot sizes and lower irradiance.

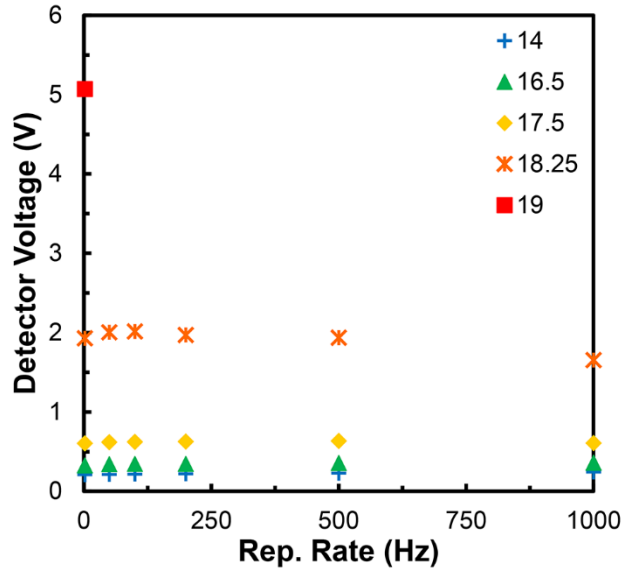


Figure 6. Measured transmitted light signal versus repetition rate (Hz) for various test positions of Sample N. The sample positions for each measurement are listed in the legend.

To summarize, the minimum peak intensity failure thresholds (TW/cm²) for all investigated samples is presented in Table 3. We reiterated the type of substrate material, failure/damage and repetition type and describe the type of damage observed at the lowest intensities:

Table 3: Sample observed Failure type (see Table 1 above) and threshold peak intensities:

Sample	Material	Damage Type	Damage Threshold (TW/cm ²)	Notes
A/B	Glass	5 / F	> 2.7	No Damage
C	Glass	5 / F	> 2.7	No Damage
D	Glass	5 / F	> 2.7	No Damage
E	Glass	5 / F	> 2.7	No Damage
F	Acrylic	2 / B	0.5	Bleaches at > 2 Hz
G	Polycarbonate	2 / A	0.5	Melt at 1 KHz

H	Polycarbonate	4 / B	N/A	OD too low
I	Polycarbonate	4 / B	1.4	Melt/Burn
J	Glass	5 / F	> 2.7	No Damage
K	Glass	5 / F	> 2.7	No Damage
L	Glass	5 / F	> 2.7	No Damage
M	Polycarbonate	4 / B	2.7	Bleaches at > 2 Hz
N	Polycarbonate	2 / A	2.7	Permanent Bleach
O	Polycarbonate	2 / A	0.014	Bleaches at > 2 Hz
P	Polycarbonate	3 / B	0.8	Damage at 1 KHz
Q	Polycarbonate	4 / B	1.4	Meling > 100 Hz
R	Polycarbonate	4 / B	0.5	Melt/Burn
U	Polycarbonate	4 / B	0.5	Melt/Burn
V	Polycarbonate	4 / A	0.5	Melt/Burn

V. CONCLUSIONS

Overall, the glass samples investigated in this study performed significantly better than the plastic dye-containing samples when tested under the same experimental conditions. None of the supplied glass samples exhibited failure under any of the test conditions while all the plastic samples failed in some manner under various laser irradiance levels. Further testing is necessary to determine why the dyes used in the plastic samples apparently fail more easily than the absorbers used in the glass substrate samples. These findings suggest that polycarbonate or acrylic eyewear, which undergo failure in various ways depending on irradiance and repetition rate, are less reliable and safe from the possibility of a direct hit from the amplified laser output. Since bleaching behavior was also commonly found, further work needs

to be performed to determine why dyes encased in plastic substrates deteriorate under high intensity illumination.

ACKNOWLEDGMENTS

We wish to thank the five anonymous laser eyewear manufacturers for graciously providing test samples for this study. Per the National Institute of Standards and Technology's requirement for anonymity, we do not identify any sources or materials but demonstrate to the laser community that different eyewear filters exhibit varying degrees of protection depending on the ultrafast laser source used and its specific output characteristics. Special thanks to Leon Lu and Jared Wahlstrand for helping make beam profile measurements. This work was partially funded by the Hood College Summer Research Institute program. The National Institute of Standards and Technology provided the lab space, Scientific Technical Research Support (STRS), and all laser and optical equipment to perform this investigation.

References

1. Stromberg, C. J.; Hadler, J. A.; Alberding, B. G.; Heilweil, E. J., "Ultrafast laser eyewear protection: Measurements and precautions," *Journal of Laser Applications* **2017**, 29 (4), 042003.
2. Miklós Lenner; Andreas Fiedler and Christian Spielmann, "Reliability of laser safety eye wear in the femtosecond regime," *Optics Express* **2004**, 12 (7), 1329; Miklós Lenner and C. Spielmann, "Protective materials for subpicosecond Ti:Sapphire lasers," *Applied Optics* **2005**, 44, 3532; Jorg Kruger and C. Spielmann, "Femtosecond laser technology in use: Safety aspects," *LTj* **2008**, 1 (Wiley-YCH Verlag GmbH and Co.),
<https://onlinelibrary.wiley.com/doi/pdf/10.1002/latj.200790209>; A. Schirmacher, a_ E. Sutter, O. Werhahn, U. Siegner, and A. Nevejina-Sturhan, "Investigation of the irradiance-dependent spectral transmittance of laser filters in the nanosecond- and femtosecond-pulse regime in the wavelength range between 700 and 800 nm," *J. Laser Applications* **17**, 191-197 (2005).

3. See European EN 207 and EN 60825 Personal Protection Equipment, Laser Safety Standards:
<http://www.hse.gov.uk/foi/internalops/oms/2009/03/om200903app3.pdf>
4. Certain commercial equipment or materials are identified in this paper to adequately specify the experimental procedures. In no case does the identification imply recommendation or endorsement by NIST, nor does it imply that the materials or equipment identified are necessarily the best available for the purpose.

Femtosecond Laser Eyewear Protection: Measurements and Precautions for Amplified High Power Applications

Maximilian Riedel-Topper, Sarah Wirick, Joshua A. Hadler,² Brian G. Alberding³
Christopher J. Stromberg¹ and Edwin J. Heilweil³

¹ Department of Chemistry and Physics, Hood College, 401 Rosemont Ave, Frederick, MD 21710

² Applied Physics Division, Physical Measurement Laboratory, NIST Boulder, CO 80305

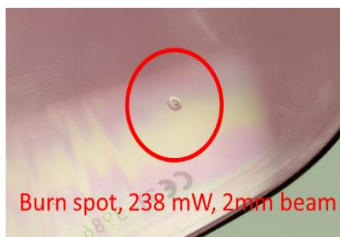
³ Engineering Physics Division, Physical Measurement Laboratory, NIST Gaithersburg, MD 20899

Supplementary Information

Diode Laser Eyewear used in Ti:Sapphire Laboratory

Rated:

190-380 nm OD > 7
755-855 nm OD > 4
780-840 nm OD > 7



$\lambda_{\text{max}} = 800 \text{ nm}$	$\text{OD}_{\text{meas}} = 7.9$
$\lambda_{\text{max}} = 792 \text{ nm}$	$\text{OD}_{\text{meas}} = 5.1$
$\lambda_{\text{max}} = 847 \text{ nm}$	$\text{OD}_{\text{meas}} = 2.5$

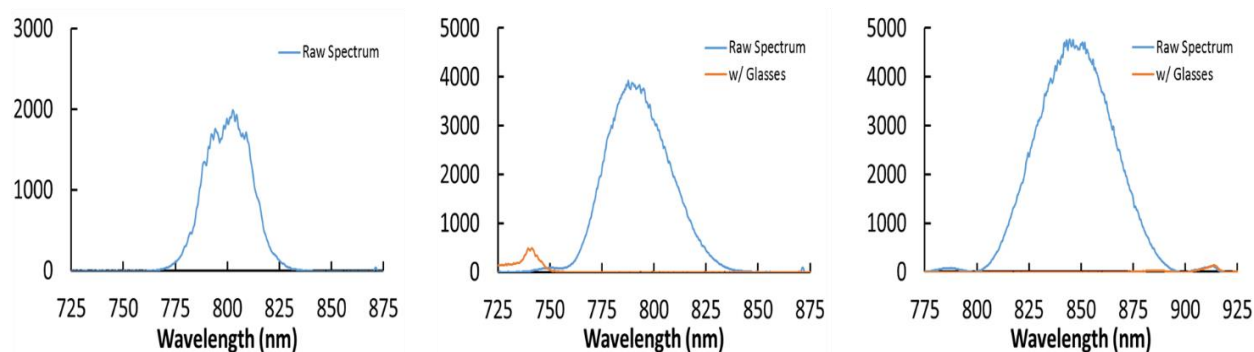


Figure S1: Sample spectral data and optical density ratings for a pair of diode laser eyewear used in the Ti:Sapphire laser laboratory. The rated optical densities at the specified wavelength ranges are shown and measured OD values for central wavelengths depicted in the spectra provided. The blue spectra are the laser output while red spectra are transmitted through the test eyewear (all arbitrary intensity scales). Note the burn spot produced at 238 mW incident with a 2 mm diameter beam. Taken from Stromberg et al, J. Laser Applications, 29, 042003 (2017).

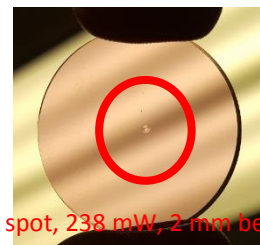
Laser Eyewear Test Sample “N”

Rated (nm):

180-390 OD > 6

785-830 OD > 5

800-818 OD > 6



Burn spot, 238 mW, 2-mm beam

$\lambda_{\text{max}} = 800 \text{ nm}$ OD_{meas} = 5.3

$\lambda_{\text{max}} = 792 \text{ nm}$ OD_{meas} = 3.9

$\lambda_{\text{max}} = 847 \text{ nm}$ OD_{meas} = 1.9

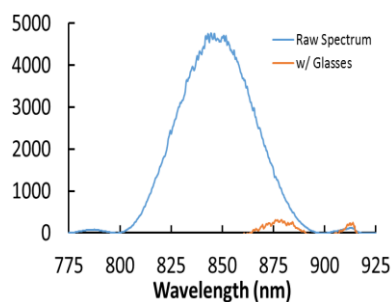
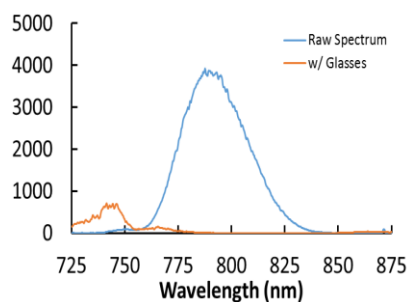
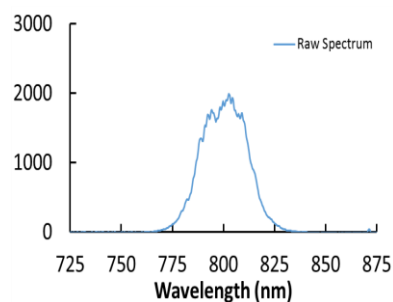
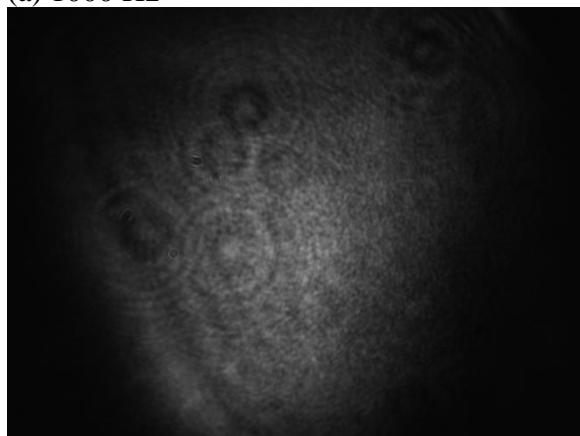
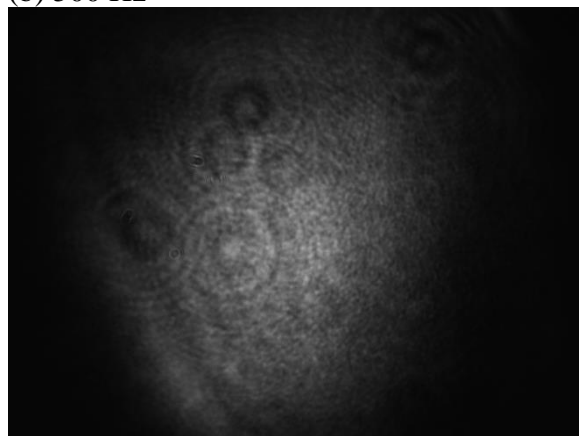


Figure S2: Test sample “N”, round plastic filter showing manufacturer’s rated optical density values for specified wavelength ranges and measured OD at center wavelengths shown in the three spectra. The blue spectrum is the raw laser output while the red spectrum is transmitted through the sample (arbitrary scales). Note this sample burned with 238 mW incident power and 2 mm beam diameter. Taken from Stromberg et al, J. Laser Applications, 29, 042003 (2017).

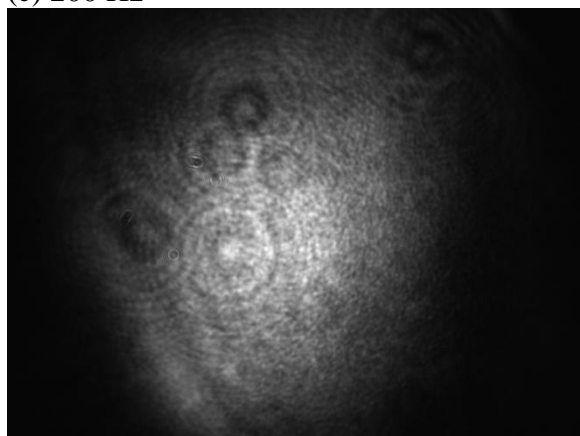
(a) 1000 Hz



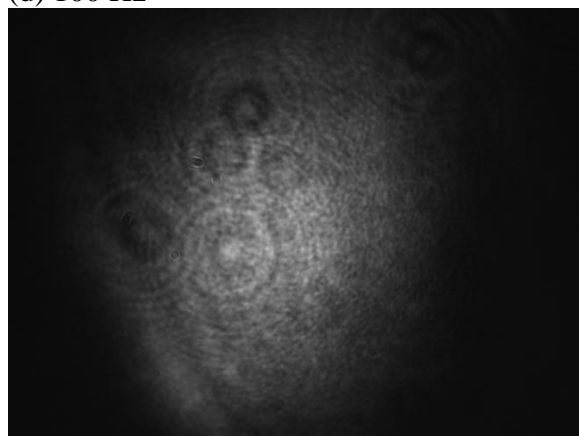
(b) 500 Hz



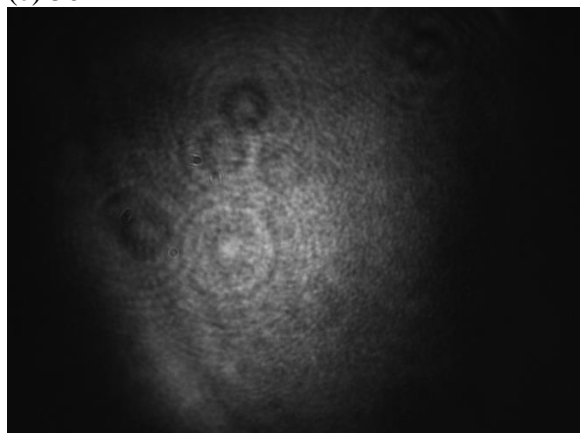
(c) 200 Hz



(d) 100 Hz



(e) 50 Hz



(f) 2 Hz

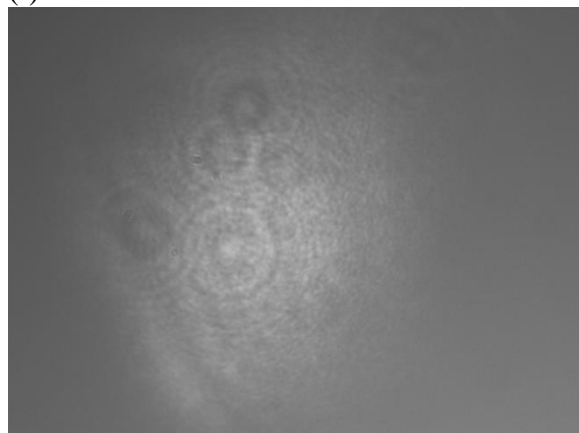
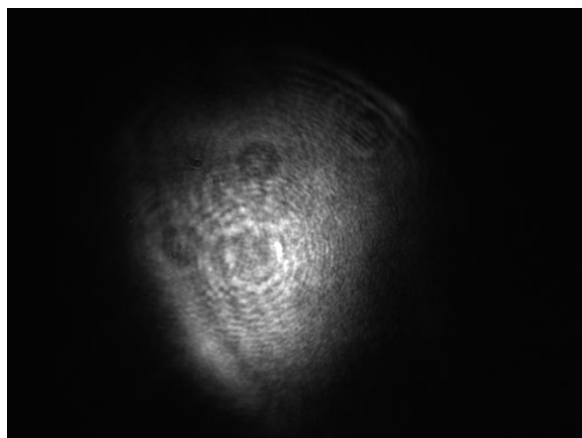


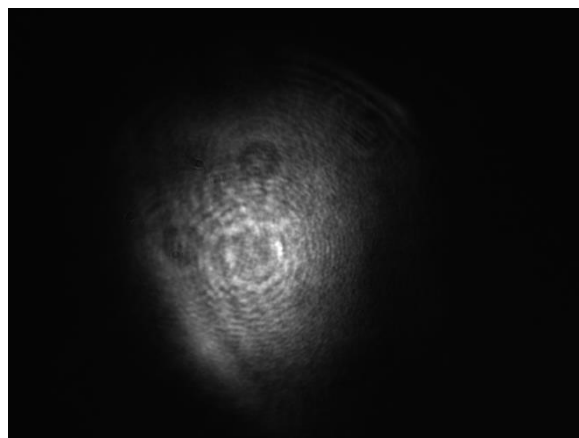
Figure S3. Photographs of beam at sample position 14.0. Repetition rates are (a) 1000 Hz, (b) 500 Hz, (c) 200 Hz, (d) 100 Hz, (e) 50 Hz, and (f) 2 Hz.

(a) 1000 Hz

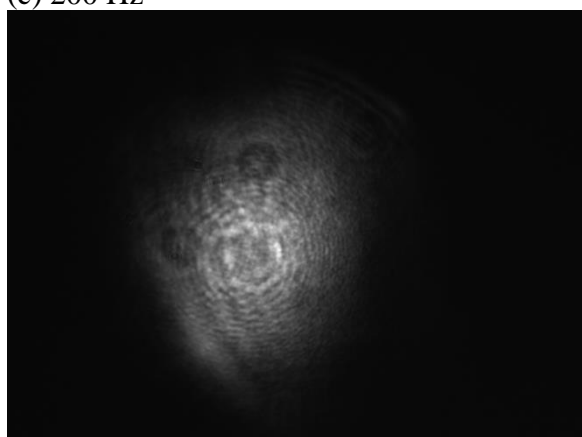
(b) 500 Hz



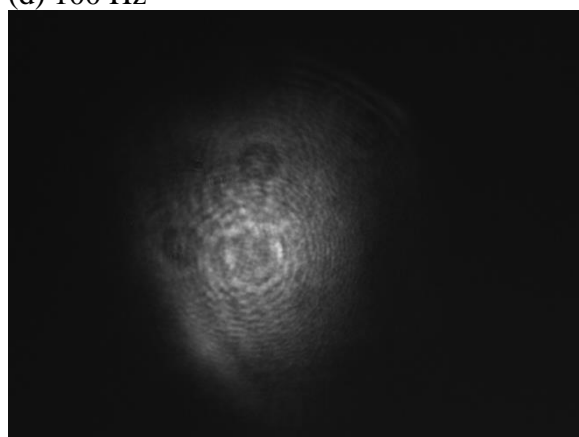
(c) 200 Hz



(d) 100 Hz



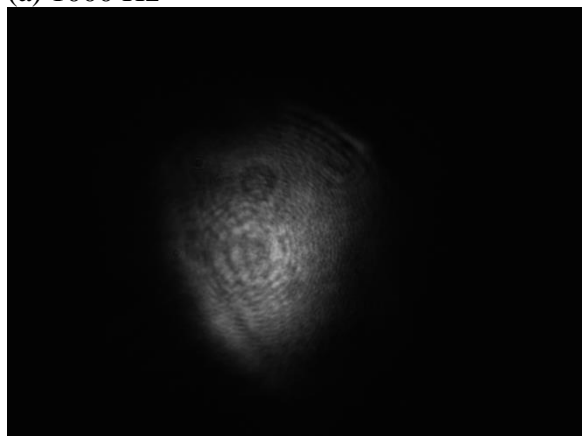
(e) 50 Hz



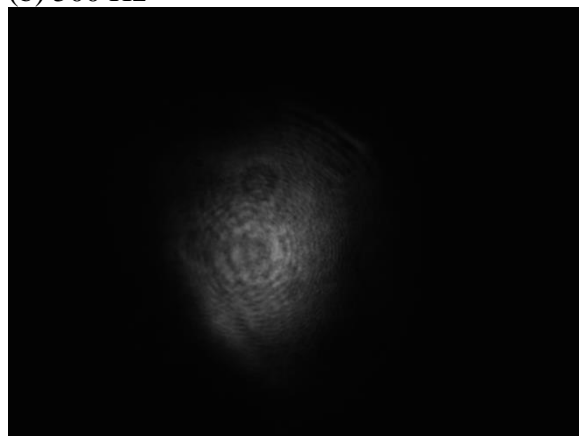
(f) 2 Hz

Figure S4. Photographs of beam at sample position 16.5. Repetition rates are (a) 1000 Hz, (b) 500 Hz, (c) 200 Hz, (d) 100 Hz, (e) 50 Hz, and (f) 2 Hz.

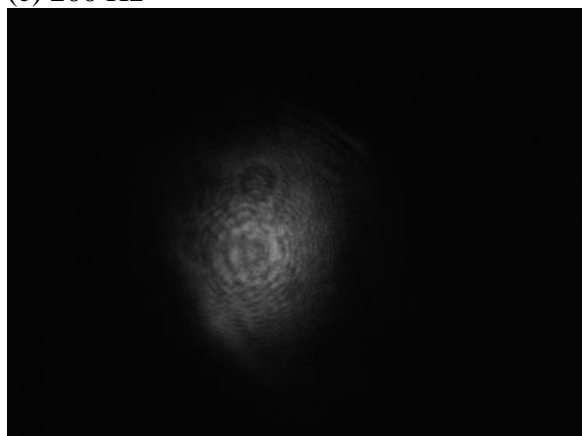
(a) 1000 Hz



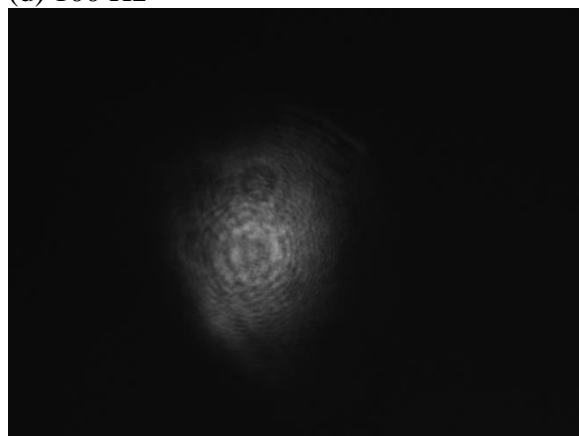
(b) 500 Hz



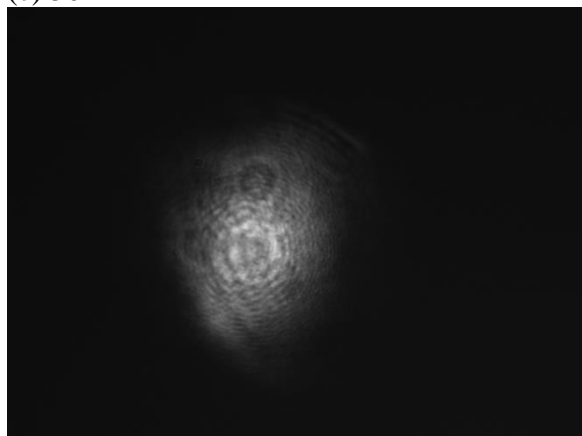
(c) 200 Hz



(d) 100 Hz



(e) 50 Hz



(f) 2 Hz

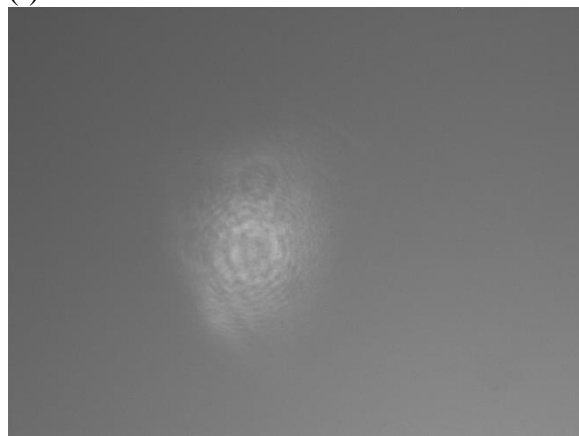
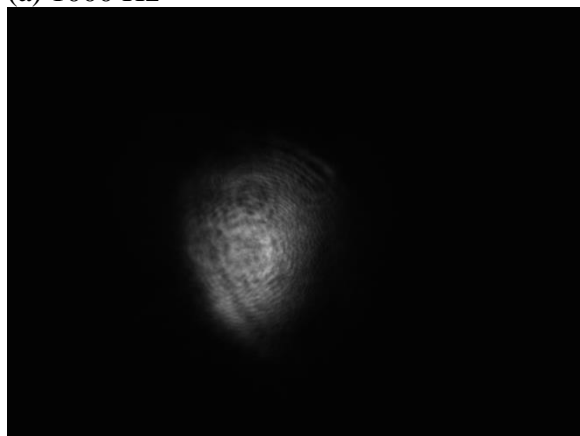
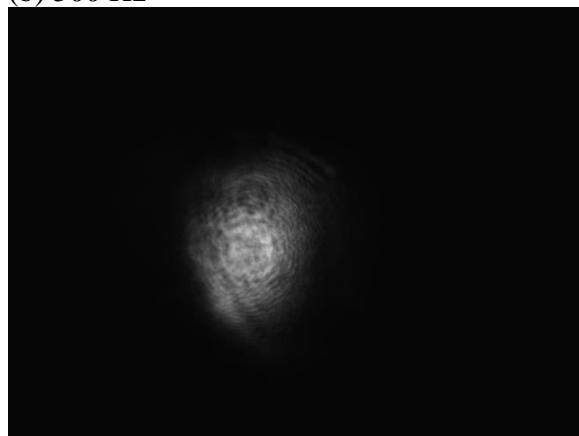


Figure S5. Photographs of beam at sample position 17.5. Repetition rates are (a) 1000 Hz, (b) 500 Hz, (c) 200 Hz, (d) 100 Hz, (e) 50 Hz, and (f) 2 Hz.

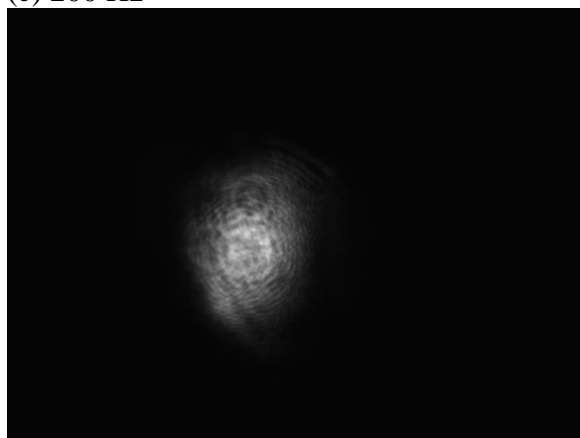
(a) 1000 Hz



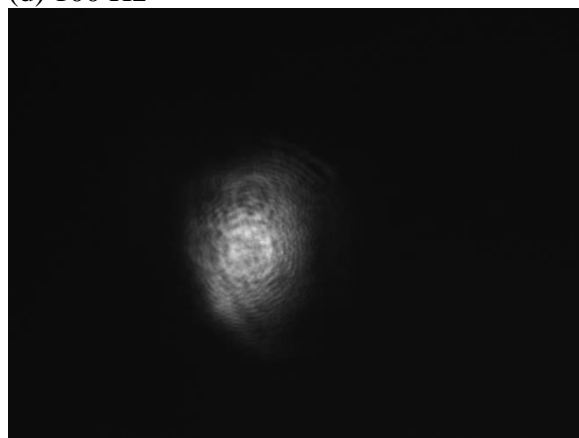
(b) 500 Hz



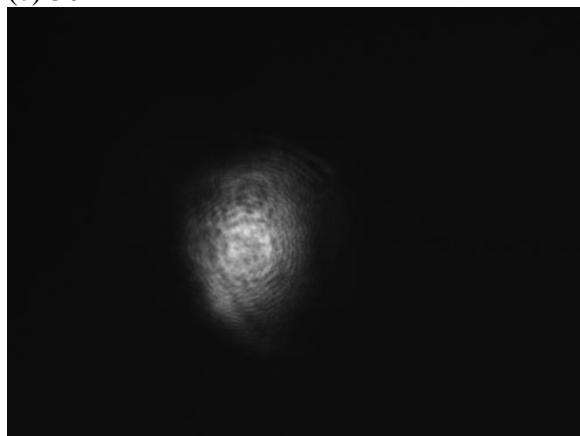
(c) 200 Hz



(d) 100 Hz



(e) 50 Hz



(f) 2 Hz

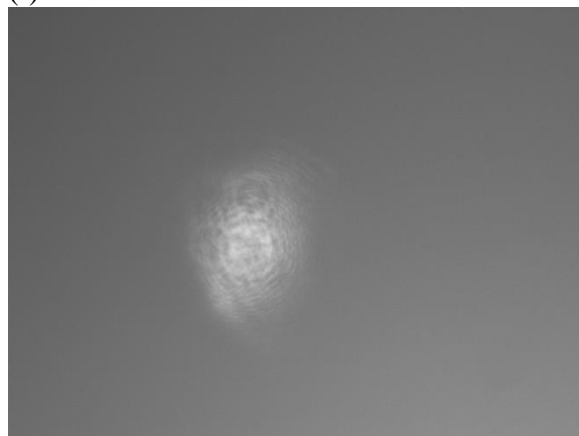
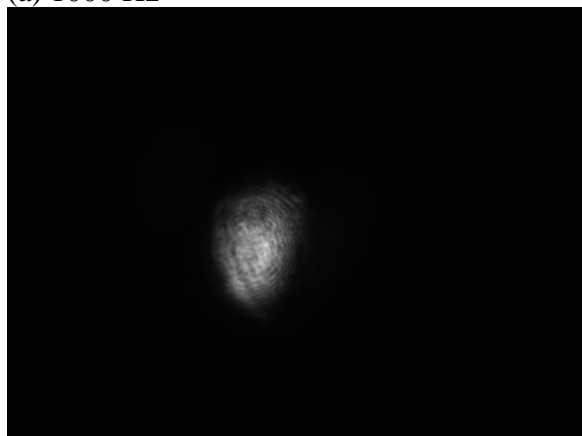
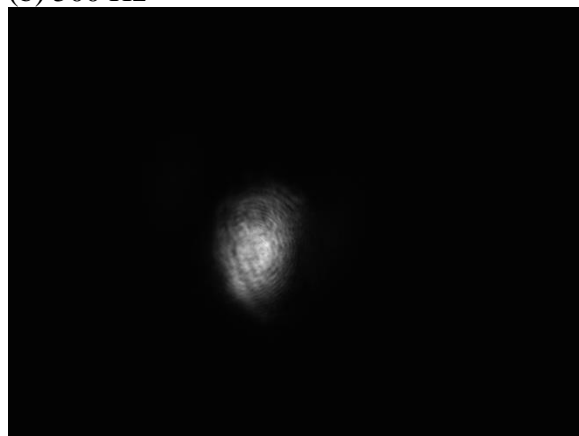


Figure S6. Photographs of beam at sample position 18.25. Repetition rates are (a) 1000 Hz, (b) 500 Hz, (c) 200 Hz, (d) 100 Hz, (e) 50 Hz, and (f) 2 Hz.

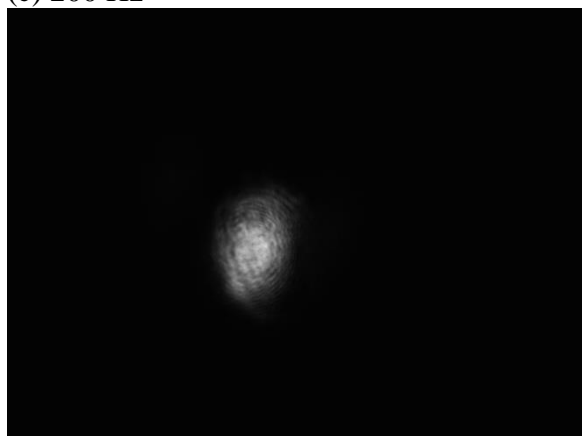
(a) 1000 Hz



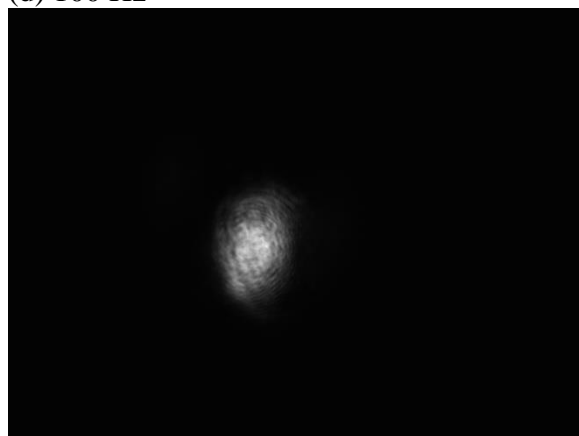
(b) 500 Hz



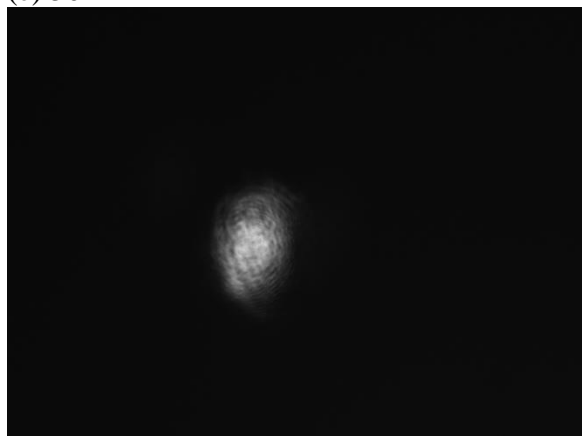
(c) 200 Hz



(d) 100 Hz



(e) 50 Hz



(f) 2 Hz

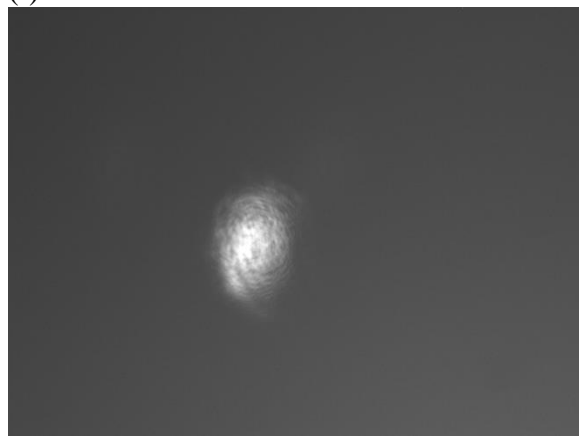


Figure S7. Photographs of beam at sample position 19.0. Repetition rates are (a) 1000 Hz, (b) 500 Hz, (c) 200 Hz, (d) 100 Hz, (e) 50 Hz, and (f) 2 Hz.